THE EUROPEAN
PHYSICAL JOURNAL C

Cosmic evolution in DHOST theory with scaling solutions

Wittaya Thipaksorn[1,a], **Khamphee Karwan**[1,2,b]

[1] The Institute for Fundamental Study "The Tah Poe Academia Institute", Naresuan University, Phitsanulok 65000, Thailand
[2] Thailand Center of Excellence in Physics, Ministry of Higher Education, Science, Research and Innovation, 328 Si Ayutthaya Road, Bangkok 10400, Thailand

Abstract   We study cosmic evolution based on the fixed points in the dynamical analysis of the degenerate higher-order scalar-tensor (DHOST) theories. We consider the DHOST theory in which the propagation speed of gravitational waves is equal to the speed of light, the tensor perturbations do not decay to dark energy perturbations, and the scaling solutions exist. The scaling fixed point associated with late-time acceleration of the universe can be either stable or saddle depending on the parameters of the theory. For some ranges of the parameters, this scaling fixed point and field-dominated fixed point can be simultaneously stable. Cosmic evolution will reach either the scaling attractor or the field-dominated attractor depending on the sign of the time derivative of the scalar field in the theory during the matter domination. The density parameter of dark matter can be larger than unity before reaching the scaling attractor if the deviation from Einstein's theory of gravity is too large. For this DHOST theory, stabilities of ϕ-matter-dominated epoch (ϕMDE) and field-dominated solutions are similar to the coupled dark energy models in Einstein gravity even though gravity is described by different theories. In our consideration, the universe can only evolve from the ϕMDE regime to the field-dominated regime. The ghost and gradient instabilities up to linear order in cosmological perturbations have been investigated. There is no gradient instability, while the ghost instability can be avoided for some range of the model parameters.

1 Introduction

Observed cosmic acceleration [1,2] is an important puzzle in modern cosmology which can possibly be explained by supposing that the physics of gravity deviates from the Einstein theory on cosmic scales [3]. Deviation from the Ein-

stein theory can be achieved if there are extra degrees of freedom for gravity in addition to two tensor degrees of freedom. For the simplest case, these extra degrees of freedom can be scalar degrees of freedom, which can be explained by a class of theories called the scalar-tensor theories of gravity [4–11]. Degenerate higher-order scalar-tensor (DHOST) theories, which are the most general scalar-tensor theories of gravity, are constructed by demanding that the theories are degenerate to eliminate Ostrogradsky instability [12–16]. This class of theories consists of a single scalar and two tensor degrees of freedom for gravity, similar to the usual Brans-Dicke theory.

The important constraint on the DHOST theories comes from the propagation speed of gravitational waves (GW), which coincides with the speed of light to an accuracy of 10^{-15} [17]. The propagation speed of GW was measured from the detection of GW and gamma-ray bursts from the merging of a binary system of neutron stars [18–21]. If the propagation speed of GW is required to be always equal to the speed of light, the action for scalar-tensor theories of gravity is tightly constrained [22–29]. For the Horndeski action, the non-minimal coupling term that satisfies this constraint is in the form of the generalized Brans-Dicke theory. The action beyond Horndeski theories [11] that satisfies the GW constraint was discussed and cosmology in this constrained theory was analyzed in [30]. The cosmic evolution and density perturbation in the DHOST theories which satisfy the constraint on the propagation speed of GW have been studied in various aspects, e.g., [31–34]. In addition to the constraint on propagation speed, we demand that GW do not decay to dark energy perturbations [35]. This requirement, together with the constraint on propagation speed of GW, tightly constrains the form of the Lagrangian for the DHOST theories. The Vainshtein mechanism for a class of DHOST theories that satisfies these two constraints was studied in [36].

Scaling and tracking behaviors for the cosmic evolution are interesting features that arise in some models of dark

Springer

energy and modified theories of gravity, because they could lead to attractors in the phase space of the cosmic evolution which could satisfy the observational constraints [37–44]. A model having scaling behavior can be obtained by assuming interaction between dark energy and dark matter. Because of this interaction, a ratio of the energy density of dark energy to that of dark matter is constant with time during the scaling regime. The scaling behavior in the interacting dark energy models has been widely investigated in the literature [45–48], and scaling and tracking solutions in the DHOST theory which satisfy the above two constraints on GW have been discussed. Demanding that the scaling and tracking solutions exist, a suitable form of the Lagrangians has been derived [49].

In this work, we analyze the stabilities of the fixed points found in [49] and discuss cosmic evolution based on these fixed points. We also explore the conditions for avoiding ghost and gradient instabilities in the class of DHOST theories.

In Sect. 2, we review the DHOST theory that has scaling solutions. The fixed points of the cosmic evolution and their stabilities are analyzed in Sect. 3, and the possible cosmic evolution associated with these fixed points is discussed. In Sect. 4, we study the stability of linear cosmological perturbations around the cosmological background. We conclude in Sect. 5.

2 DHOST theories with scaling solutions

2.1 Review of DHOST theories

The DHOST theories are constructed by imposing the degeneracy conditions to the most general form of the Lagrangian containing second-order derivatives of the scalar field in the form

$$L = G_2(\phi, X) + G_3(\phi, X)\Box\phi + G_4(\phi, X)R + C_{(2)}^{\alpha\beta\mu\nu}\phi_{\alpha\beta}\phi_{\mu\nu} + C_{(3)}^{\alpha\beta\mu\nu\rho\sigma}\phi_{\alpha\beta}\phi_{\mu\nu}\phi_{\rho\sigma}, \tag{1}$$

where R is the Ricci scalar, $X \equiv -\phi_\mu\phi^\mu$, $\phi_\mu \equiv \nabla_\mu\phi$, $\phi_{\mu\nu} \equiv \nabla_\nu\nabla_\mu\phi$, and ∇_ν denotes a covariant derivative compatible with the metric $g_{\mu\nu}$. In the following consideration,

we concentrate on the terms up to the quadratic in the second-order derivatives of the scalar field. The possible form of the quadratic terms can be written as [12]

$$C_{(2)}^{\alpha\beta\mu\nu}\phi_{\alpha\beta}\phi_{\mu\nu} = A_1(\phi, X)\phi_{\mu\nu}\phi^{\mu\nu} \\ + A_2(\phi, X)(\Box\phi)^2 + A_3(\phi, X)\Box\phi\,\phi^\mu\phi_{\mu\nu}\phi^\nu \\ + A_4(\phi, X)\phi^\mu\phi_{\mu\rho}\phi^{\rho\nu}\phi_\nu \\ + A_5(\phi, X)(\phi^\mu\phi_{\mu\nu}\phi^\nu)^2. \tag{2}$$

Based on the degeneracy conditions, the DHOST theories can be classified into three classes. However, the theories in class I can be free from the gradient instability, while those in class II cannot, because the square of the sound speed of the tensor and scalar perturbations have opposite signs [50,51] For class III, the tensor degrees of freedom do not propagate. Hence, we concentrate on class I. The degeneracy conditions for class I are

$$A_2 = -A_1, \tag{3}$$

$$A_4 = -A_3 + \frac{(-4G_{4X} - 2A_1 - XA_3)\left(-12G_4G_{4X} - 6A_1G_4 - 8A_1^2X + A_3G_4X - 16A_1G_{4X}X\right)}{8(G_4 + XA_1)^2}, \tag{4}$$

$$A_5 = \frac{(-4G_{4X} - 2A_1 - XA_3)\left(-2A_1^2 + 3XA_1A_3 - 4G_{4X}A_1 + 4G_4A_3\right)}{8(G_4 + XA_1)^2}, \tag{5}$$

where subscript X denotes the derivative with respect to X. For the DHOST theories which depend quadratically on second-order derivatives of the scalar field, the propagation speed of the tensor perturbations is given by [52]

$$c_T^2 = \frac{G_4}{G_4 + XA_1}, \tag{6}$$

where the speed of light is equal to unity in this expression. From the Laser Interferometer Gravitational-Wave Observatory (LIGO)/Virgo results [17,49,53], c_T is equal to the speed of light, so that Eq. (6) yields

$$A_1 = 0. \tag{7}$$

It has been shown that the GW in DHOST theories can decay to scalar perturbations. To avoid this decay, we demand [35]

$$A_3 = 0. \tag{8}$$

Inserting the conditions from Eqs. (7) and (8) into Eqs. (4) and (5), we get

$$A_5 = 0, \quad \text{and} \quad A_4 = \frac{6G_{4X}^2}{G_4}. \tag{9}$$

Hence, the action for quadratic DHOST theories in which the propagation speed of GW is equal to the speed of light

and the GW do not decay to dark energy perturbations can be written in the form

$$S_G = \int d^4x \sqrt{-g} \left\{ G_2 + G_3 \Box\phi + G_4 R + \frac{6G_{4X}^2}{G_4} \phi^\mu \phi_{\mu\rho} \phi^{\rho\nu} \phi_\nu \right\}, \tag{10}$$

where we have set the reduced Planck mass $M_p \equiv 1/\sqrt{8\pi G} = 1$. The G_3 term will be dropped in the following consideration for simplicity. The above action can also be obtained by applying a conformal transformation in which the transformation coefficient depends on both a scalar field and its kinetic term to the Einstein–Hilbert action [54]. We write the total action as

$$S = S_G + S_M. \tag{11}$$

Here, S_M is the action for the matter in the universe including ordinary matter and dark matter. The ordinary matter is minimally coupled to gravity, while the dark matter is coupled non-gravitationally to scalar field ϕ and coupled non-minimally to gravity. The action for dark matter is denoted by S_m in the following sections.

2.2 Evolution equations for the background universe

To study the evolution of the background universe in the DHOST theories described by the action (11), we use the Friedmann–Lemaître–Robertson–Walker (FLRW) metric for the spatially flat universe in the form

$$ds^2 = -n^2(t)dt^2 + a^2(t)\delta_{ij}dx^i dx^j, \tag{12}$$

where δ_{ij} is the Kronecker delta, $a(t)$ is the cosmic scale factor, and $n(t)$ is an auxiliary function which will be set to unity after the evolution equations are obtained. Using the above line element and homogeneity of the scalar field in the background universe, the action (11) becomes

$$S = \int dt\, a^3 n$$
$$\times \left\{ G_2 - 6G_{4\phi} H \frac{\dot\phi}{n^2} - 6G_4 \left[\frac{H}{n} + \frac{G_{4X}}{G_4} \frac{\dot\phi}{n^2} \frac{d}{dt}\left(\frac{\dot\phi}{n}\right) \right]^2 \right\} + S_M, \tag{13}$$

where a dot denotes derivative with respect to time t, $H \equiv \dot a/a$ is the Hubble parameter, and subscript $_\phi$ denotes the derivative with respect to ϕ.

Variations in the action (13) with respect to n and a yield

$$\rho_M = E_{00} \equiv \frac{1}{G_4^2} \left[-G_4 X \left(-6\dot\phi \left(-2G_{4X}^2 \dddot\phi - 6HG_{4X}^2 \ddot\phi \right) \right. \right.$$
$$\left. + G_4 \left(12\left(2H^2 + \dot H\right) G_{4X} + 2G_{2X} \right) + 6G_{4X}^2 \ddot\phi^2 \right)$$
$$\left. + G_4^2 \left(6G_4 H^2 + 6H\dot\phi \left(2G_{4X}\ddot\phi + G_{4\phi} \right) + G_2 \right) \right.$$

$$+ 12X^2 G_{4X} \ddot\phi \left(\left(G_{4X}^2 - 2G_4 G_{4XX} \right) \ddot\phi \right.$$
$$\left. - 2G_4 G_{4\phi X} + G_{4X} G_{4\phi} \right) \Big], \tag{14}$$

and

$$-p_M = E_{ii} \equiv \frac{1}{G_4} \left[G_4 \left(4\dot\phi \left(G_{4X}\dddot\phi + 2HG_{4X}\ddot\phi + HG_{4\phi} \right) \right. \right.$$
$$\left. + 6G_4 H^2 + 4G_4 \dot H + 4G_{4X}\ddot\phi^2 + 2G_{4\phi}\ddot\phi + G_2 \right)$$
$$+ X \left(\left(8G_4 G_{4XX} - 6G_{4X}^2 \right) \ddot\phi^2 \right.$$
$$\left. \left. + 8G_4 \ddot\phi G_{4\phi X} + 2G_4 G_{4\phi\phi} \right) \right], \tag{15}$$

where ρ_M and p_M are the energy density and pressure of the total matter, in which each of the matter components is perfect fluid. These quantities can be obtained by varying the action S_M with respect to the metric. Equations (14) and (15) together with Eq. (20) agree with Eqs. (2.13) and (2.14) in [49]. These two equations can be combined to eliminate $\dot H$ as

$$0 = \frac{1}{G_4^2} \left[G_4 X \left(-6G_4 H^2 G_{4X} + 6H\dot\phi \left(2G_{4X}G_{4\phi} - 2G_{4X}^2 \ddot\phi \right) \right. \right.$$
$$\left. + 6G_{4X}^2 \ddot\phi^2 + 6G_{4X}G_{4\phi}\ddot\phi - 2G_4 G_{2X} + 3G_2 G_{4X} \right)$$
$$+ G_4^2 \left(6G_4 H^2 + 6H\dot\phi \left(2G_{4X}\ddot\phi + G_{4\phi} \right) + G_2 \right)$$
$$- G_4 \rho_M \left(G_4 - 3XG_{4X}w_M \right)$$
$$\left. + 3X^2 G_{4X} \left(-2G_{4X}^2 \ddot\phi^2 + 4G_{4X}G_{4\phi}\ddot\phi + 2G_4 G_{4\phi\phi} \right) \right]. \tag{16}$$

In the above equation, $w_M \equiv p_M/\rho_M$ is the equation-of-state parameter of the total matter, which is not necessarily zero. Varying the action (13) with respect to the scalar field ϕ, we obtain the evolution equation for the scalar field, which can be written in the form

$$F(\ddddot\phi, \dddot\phi, \ddot\phi, \dot\phi, \phi, \ddot H, \dot H, H) = Q, \tag{17}$$

where Q is the interaction term arising from the variation in the action S_m for dark matter with respect to the scalar field ϕ. We will see in the following sections that the coupling between the scalar field and matter is needed for shifting the effective equation-of-state parameter $w_{\text{eff}} \equiv w_\phi \Omega_\phi$ during the scaling regime at late time to a negative value as required by observations. Here, w_ϕ and Ω_ϕ are the effective equation-of-state parameter and effective density parameter of scalar degrees of freedom associated with the scalar field ϕ defined below. In the following consideration, we suppose that the interaction term Q is a consequence of an energy transfer between the scalar field and dark matter. In principle, the form of the interaction term Q depends on the form of S_m. However, for simplicity, we start with the phenomenological form of the interaction term studied in the literature. We write the function F in the above equation in the form of the conservation equation for the effective energy density of the scalar field as $F \to \dot\rho_\phi + 3H(\rho_\phi + p_\phi) = 0$. Then we add the phenomenological interaction term on the right-hand side of

the conservation equation as

$$\dot{\rho}_\phi + 3H(\rho_\phi + p_\phi) = -Q\rho_m\dot{\phi}, \tag{18}$$

where Q is constant, and ρ_ϕ and p_ϕ are the effective energy density and effective pressure of the scalar field ϕ. Supposing that the total energy density of the scalar field and dark matter is conserved, we have

$$\dot{\rho}_m + 3H\rho_m = Q\rho_m\dot{\phi}, \tag{19}$$

where a subscript $_m$ denotes the quantities for dark matter. The effective energy density and pressure of the scalar field are defined such that Eqs. (14) and (15) take the forms of the usual Friedmann and acceleration equations as $3H^2 = \rho_M + \rho_\phi$ and $2\dot{H} + 3H^2 = -p_M - p_\phi$. The expressions for ρ_ϕ and p_ϕ can be read from Eqs. (14) and (15) as

$$\rho_\phi \equiv 3H^2 - E_{00}, \quad p_\phi \equiv E_{ii} - 2\dot{H} - 3H^2. \tag{20}$$

From the above expressions, the effective equation-of-state parameter of the scalar field can be defined as $w_\phi \equiv p_\phi/\rho_\phi$. According to the definitions of p_ϕ and ρ_ϕ, we can write

$$\begin{aligned} \frac{\dot{H}}{H^2} &= -\frac{3}{2}\left(1 + \Omega_M w_M + \Omega_\phi w_\phi\right) \\ &= -\frac{3}{2}\left(1 + \frac{1}{3}\Omega_\gamma + w_{\text{eff}}\right). \end{aligned} \tag{21}$$

Here, Ω_γ is the density parameter of radiation, where $\Omega_M = \Omega_m + \Omega_\gamma$, and Ω_m is the density parameter of dark matter. The evolution of the background universe can be studied using dynamical analysis. To compute the autonomous equations describing the evolution of the background universe, we have to know the expression for the ratio $\dot{H}/H^2$. To compute this ratio, we firstly differentiate Eq. (15) with respect to time. Then we eliminate $\dddot{\phi}$ from the resulting equation using Eq. (17). The remaining $\dddot{\phi}$ terms can be eliminated using Eq. (15). Finally, we obtain

$$0 = \tilde{E}_i(\ddot{\phi}, \dot{\phi}, \phi, H, \rho_m). \tag{22}$$

Differentiating the above equation with respect to time and eliminating $\dddot{\phi}$ terms using Eq. (15), we obtain

$$\frac{\dot{H}}{H^2} = -h(\ddot{\phi}, \dot{\phi}, \phi, H, \rho_m). \tag{23}$$

2.3 Scaling solutions

The gravity theories described by the action (13) can have scaling behavior if the effective energy density and effective pressure of the scalar field together with the energy density of the matter obey the scaling relations $\rho_\phi \propto p_\phi \propto \rho_m \propto H^2$. During the scaling regime, we have

$$\frac{\dot{\phi}}{H} = \frac{2h}{\lambda} = \text{constant}. \tag{24}$$

Based on the analysis in [49], for constant coupling Q, the DHOST theory in action (13) has scaling solutions if

$$G_2 = X g_2(Y) \quad G_4 = \frac{1}{2} + g_4(Y), \tag{25}$$

where G_2 and G_4 are arbitrary functions of

$$Y = \frac{X e^{\frac{\lambda\phi}{M_p}}}{M_p^4}. \tag{26}$$

Here, λ is constant and M_p is restored in the above expression and some subsequent relations to avoid confusion. To study scaling solutions in DHOST theories, we set G_2 and G_4 according to Eq. (25). Since Y is a linear function of the kinetic term X, we choose G_2 and G_4 as polynomial functions of Y [49]:

$$G_2 = X\left(\tilde{c}_2 Y^{n_2} - \tilde{c}_6 Y^{n_6}\right), \tag{27}$$

$$G_4 = \frac{1}{2} + \tilde{c}_4 Y^{n_4}, \tag{28}$$

where $\tilde{c}_2$, $\tilde{c}_4$ and $\tilde{c}_6$ are constant, and n_2, n_4 and n_6 are constant integers. The above expressions for G_2 and G_4 are mainly motivated by demanding scaling solutions in the model. Additional motivation for these choices of G_2 and G_4 are based on the requirement that G_2 can reduce to a form of the Lagrangian for the canonical scalar field if $n_2 = 0$ and $n_6 = -1$, while G_4 can reduce to the case of the Einstein theory when $\tilde{c}_4 = 0$. Since the existence of the scaling solutions requires that G_2 and G_4 depend on the scalar field ϕ through Y, shift symmetry is broken in this scaling model, and consequently a self-accelerating solution is absent. This implies that the field ϕ is required to be slowly varying with time to drive the cosmic acceleration at late time. When the coupling between the scalar field and dark matter is constant, the scaling solutions can give

$$\lambda = -\frac{2hQ}{3\Omega_\phi w_\phi}. \tag{29}$$

3 Stabilities of the fixed points and the corresponding cosmic evolution

3.1 Autonomous equations

To compute the autonomous equations from the evolution equations in the previous section, we define the dimensionless variables as

$$x \equiv \frac{\dot{\phi}}{M_p H}, \quad y \equiv \frac{M_p^2 e^{\frac{-\lambda\phi}{M_p}}}{H^2}, \quad z \equiv \frac{\ddot{\phi}}{\dot{\phi}H}. \tag{30}$$

For convenience, we normalize the variables x, y and z by their values at scaling fixed point, such that

$$x_r \equiv \frac{x}{x_s}, \quad y_r \equiv \frac{y}{y_s}, \quad \text{and} \quad z_r \equiv \frac{z}{z_s}, \tag{31}$$

where subscript $_s$ denotes the quantities at the scaling fixed point. The scaling fixed point in this case is the fixed point that x satisfies the condition in Eq. (24) and Q satisfies Eq. (29). To compute x_s and z_s, we compute the derivative of x with respect to $N \equiv \ln a$ as

$$x' = zx - x\frac{\dot{H}}{H^2}, \tag{32}$$

which is a possible form of the autonomous equation. Here, a prime denotes a derivative with respect to N. From the condition in Eq. (24), we have

$$h_s = \left.\frac{\dot{\phi}\lambda}{2H}\right|_s \equiv \frac{x_\lambda}{2}, \tag{33}$$

where $x_\lambda \equiv x_s\lambda$. Inserting this solution into Eq. (32), we get $z_s = -h_s = -x_\lambda/2$. In terms of dimensionless variables, the constraint equations (16) and (22) are given by Eqs. (A2) and (A3) in the appendix. We see that these constraint equations can be solved for z and Ω_m in terms of x and y. Here we are interested in the evolution of the late-time universe so that we set $\Omega_\gamma = 0$. Hence, the late-time dynamics of the background universe can be described by two dynamical variables x and y.

Using definitions of x_r and y_r, we can write the autonomous equations as

$$x'_r = -\frac{x_\lambda z_r x_r}{2} - x_r\frac{\dot{H}}{H^2}, \tag{34}$$

$$y'_r = -x_\lambda x_r y_r - 2y_r\frac{\dot{H}}{H^2}, \tag{35}$$

where z_r is computed from the constraint equations whose solutions are shown in Eqs. (A5)–(A7). When the autonomous equations are written in these forms, the coupling constant Q in the autonomous equations is always divided by λ, so that the dynamics of the background universe depend on Q/λ rather than Q. In the numerical integration for the evolution of the universe discussed below, we concentrate on the case where z_r is the first solution given in Eq. (A5) to avoid contributions from the imaginary part of the solution. We note that the solutions which give $z_r = x_r = y_r = 1$ are not necessarily the solution in Eq. (A5), unless $n_4 = \pm 1$. Hence, in our numerical integration for the cosmic evolution, we set n_4 to be either -1 or 1. According to Eq. (23), $\dot{H}/H^2$ also depends on Ω_m. However, Ω_m in this expression can be eliminated using the constraint equations Eq. (A2).

To compute the fixed points of this system, we set x_r, y_r and z_r in the constraint equations Eqs. (A1) and (A2) to be unity, and then we solve for the parameters as

$$c_2 = -\frac{1}{2(2c_4 + 1)^2(n_2 - n_6)}$$
$$\left[-6c_4^2\left(-2\left(\Omega_{ms} + 2n_6(x_\lambda - 3) + x_\lambda - 6\right) + 2n_4^3x_\lambda^2\right.\right.$$
$$\left.-n_4^2x_\lambda(n_6x_\lambda + x_\lambda - 6) + 4n_4(x_\lambda - 4)\right)$$
$$+6c_4\left(2\Omega_{ms} - n_4(x_\lambda - 4) + 2n_6(x_\lambda - 3) + x_\lambda - 6\right)$$
$$-4c_4^3\left(3n_4^3x_\lambda^2 - 3n_4^2x_\lambda\right.$$
$$(n_6x_\lambda + x_\lambda - 6) + 6n_4(x_\lambda - 4) - 2(2n_6(x_\lambda - 3)$$
$$\left.+x_\lambda - 6)\right) + 3\Omega_{ms}$$
$$+2n_6(x_\lambda - 3) + x_\lambda - 6], \tag{36}$$

$$c_6 = -\frac{1}{2(2c_4 + 1)^2(n_2 - n_6)}$$
$$\left[6c_4^2\left(2\left(\Omega_{ms} + x_\lambda - 6\right)\right.\right.$$
$$-2n_4^3x_\lambda^2 + n_4^2(x_\lambda - 6)x_\lambda - 4n_4(x_\lambda - 4)$$
$$\left.+n_2\left(n_4^2x_\lambda^2 + 4x_\lambda - 12\right)\right)$$
$$+6c_4\left(2\Omega_{ms} - n_4(x_\lambda - 4) + 2n_2(x_\lambda - 3) + x_\lambda - 6\right)$$
$$-4c_4^3\left(3n_4^3x_\lambda^2 - 3n_4^2(x_\lambda - 6)x_\lambda\right.$$
$$+6n_4(x_\lambda - 4) + n_2\left(-3n_4^2x_\lambda^2 - 4x_\lambda + 12\right) - 2(x_\lambda - 6)\right)$$
$$+3\Omega_{ms} + 2n_2(x_\lambda - 3) + x_\lambda - 6], \tag{37}$$

where Ω_{ms} is Ω_m at the scaling fixed point, and we redefine the coefficients as

$$c_2 \equiv \tilde{c}_2 x_s^2 Y_s^{n_2}, \quad c_4 \equiv \tilde{c}_4 Y_s^{n_4}, \quad \text{and} \quad c_6 \equiv \tilde{c}_6 x_s^2 Y_s^{n_6}. \tag{38}$$

We set $h_s = x_\lambda/2$ and $x_r = y_r = 1$, and substitute c_2 and c_6 from Eqs. (36) and (37) into Eq. (23) as

$$\frac{x_\lambda}{2} = h(\ddot{\phi}, \dot{\phi}, \phi, H, \rho_m)|_s = h(x_r, y_r, z_r, \Omega_m)|_s$$
$$= h(1, 1, 1, \Omega_{ms}). \tag{39}$$

This relation yields

$$0 = \frac{18c_4(2c_4 + 1)^4 n_4\Omega_{ms}(Q_\lambda - 2)x_\lambda^{13}(Q_\lambda x_\lambda + x_\lambda - 3)}{\lambda^{12}}, \tag{40}$$

where $Q_\lambda = Q/\lambda$. The interesting conditions required by the above equation are

$$\Omega_{ms} = 0, \quad Q_\lambda x_\lambda + x_\lambda - 3 = 0, \quad \text{or} \quad c_4 = 0. \tag{41}$$

We can see that $Q_\lambda - 2 = 0$ is the special case of the condition $Q_\lambda x_\lambda + x_\lambda - 3 = 0$. These conditions lead to three classes of fixed point as follows: (1) $Q_\lambda x_\lambda + x_\lambda - 3 = 0$ corresponding to a scaling fixed point where Q satisfies Eq. (29), (2) $\Omega_{ms} = 0$ corresponding to the field-dominated point where Q does not necessarily satisfy Eq. (29), and (3) $c_4 = 0$ yielding $y_r = 0$ for negative n_4. These fixed points have been found in [49]. The stabilities of these fixed points will be discussed in the next section.

3.2 Fixed points and stabilities

To investigate the stabilities of the fixed points, we linearize the autonomous equations around the fixed point and check the signs of the eigenvalues of the Jacobian matrix defined by

$$
J_{ij} = \left. \frac{\partial x'_i}{\partial x_j} \right|_{\text{fixed point}},
\tag{42}
$$

where $x_i = (x_r, y_r)$.

3.2.1 Scaling fixed point

The scaling fixed point corresponds to the condition

$$
x_\lambda = \frac{3}{Q_\lambda + 1}.
\tag{43}
$$

From $h_s = x_\lambda/2$, we have

$$
w_{\text{eff}} = -\frac{Q_\lambda}{Q_\lambda + 1}.
\tag{44}
$$

We see that if the coupling term disappears, $w_{\text{eff}} = 0$, because for the scaling solution, ρ_ϕ/ρ_m is constant. Using the relation $w_{\text{eff}} = \Omega_\phi w_\phi$ and Eq. (44), we can compute Ω_ϕ as well as Ω_m at the fixed point if w_ϕ at the fixed point is specified. Inserting the relations for the scaling fixed point into the Jacobian matrix, we obtain the polynomial equation for the eigenvalues of the fixed point. For sufficiently large c_4, the eigenvalues of the Jacobian matrix depend only on x_λ and are given by

$$
E_{al} = \left\{ \frac{x_\lambda - 6}{2}, 0 \right\}.
\tag{45}
$$

Since one of the eigenvalues is zero, the stability of this fixed point cannot be determined using linear stability analysis. Nonlinear stability analysis can be performed using the center manifold method, but we will not consider nonlinear analysis in this work. If c_4 is not too large, the eigenvalues of the Jacobian matrix can be written as

$$
E_a = \{\mu_1, \mu_2\}.
\tag{46}
$$

To describe the accelerated expansion of the late-time universe required by observations, we demand that $x_\lambda < 1$. The eigenvalues μ_1 and μ_2 can be computed from the equation

$$
a_2 \mu^2 + a_1 \mu + a_0 = 0,
\tag{47}
$$

where a_2, a_1 and a_0 are complicated functions of x_λ, $\Omega_{ms}, c_2, c_4, c_6, n_2, n_4$ and n_6. The solutions for the above equation can be written as

$$
\mu_1 = \frac{x_\lambda - 6}{4} \left(1 - \sqrt{1 + \frac{8a_0}{a_1(x_\lambda - 6)}} \right),
$$

$$
\mu_2 = \frac{x_\lambda - 6}{4} \left(1 + \sqrt{1 + \frac{8a_0}{a_1(x_\lambda - 6)}} \right).
\tag{48}
$$

In the above expressions, the relation $a_1/(2a_2) = (6 - x_\lambda)/4$ is used. It follows from the relations for μ_1 and μ_2 that the real part of μ_2 is always negative for $x_\lambda < 6$, while the real part of μ_1 can be either negative or positive. Hence, the fixed point is stable when the real part of μ_1 is negative and becomes saddle when the real part of μ_1 is positive. Because of the lengthy expressions for a_0, a_1 and a_2, we compute μ_1 numerically and plot the results as a function of c_4.

The real part of μ_1 for some choices of the parameters is plotted in Fig. 1. In all plots, x_λ and Ω_{ms} are chosen such that w_{eff} satisfies observational constraints. For $\Omega_{ms} = 0.3$, we set $x_\lambda = 0.92$ and $x_\lambda = 0.69$ which correspond to $w_\phi = -0.99$ and $w_\phi = -1.10$, respectively.

From Fig. 1 and Eq. (48), we see that the stability of the fixed point depends on x_λ, which controls the value of w_{eff} through the relation $x_\lambda = -3(1 + w_{\text{eff}})$. In the plot, when x_λ decreases, the fixed point of some models, e.g., the model with $n_6 = -1$, can become a saddle point. According to Fig. 1, the fixed point is stable for the wide range of c_4 if n_6 is positive. For $n_6 = -3$, the fixed point can be either saddle or stable depending on the value of c_4. From the plot, we see that the real part of μ_1 reaches zero when c_4 is sufficiently large independently of n_2, n_4, n_6 and x_λ, which agrees with Eq. (45).

### 3.2.2 Field-dominated point

Equation (40) indicates that $\Omega_m = 0$ is a possible fixed point of the system. To obtain Eq. (40), we set $h = x_\lambda/2$ at the fixed point according to Eq. (24). Nevertheless, the condition $h = x_\lambda/2$ can be relaxed if x_r, y_r and z_r are not equal to unity at a fixed point, where the condition $x_r = y_r = z_r = 1$ defines the scaling fixed point. From Eqs. (34) and (35), we see that the fixed points exist when

$$
h = \frac{x_\lambda}{2} z_r = \frac{x_\lambda}{2} x_r,
\tag{49}
$$

where the expressions for x_r and z_r at the fixed point can be solved from Eqs. (A1), (A2) and (A3). For the fixed point $\Omega_m = 0$, the expressions for x_r and z_r are complicated and strongly depend on n_2, n_4 and n_6, because Eqs. (A1), (A2) and (A3) contain $x_r^{n_2}, x_r^{n_4}$ and $x_r^{n_6}$. However, we can substitute Eq. (49) into Eq. (21) to obtain

$$
w_\phi = w_{\text{eff}} = -1 + \frac{x_\lambda x_{r\,b}}{3},
\tag{50}
$$

where subscript $_b$ denotes evaluation at the field-dominated point. We note that for this fixed point there is no requirement for Q_λ. It follows from Eqs. (18) and (19) that the effect of the coupling Q disappears when $\Omega_m = 0$. According to this fixed point, the eigenvalues computed from the Jacobian
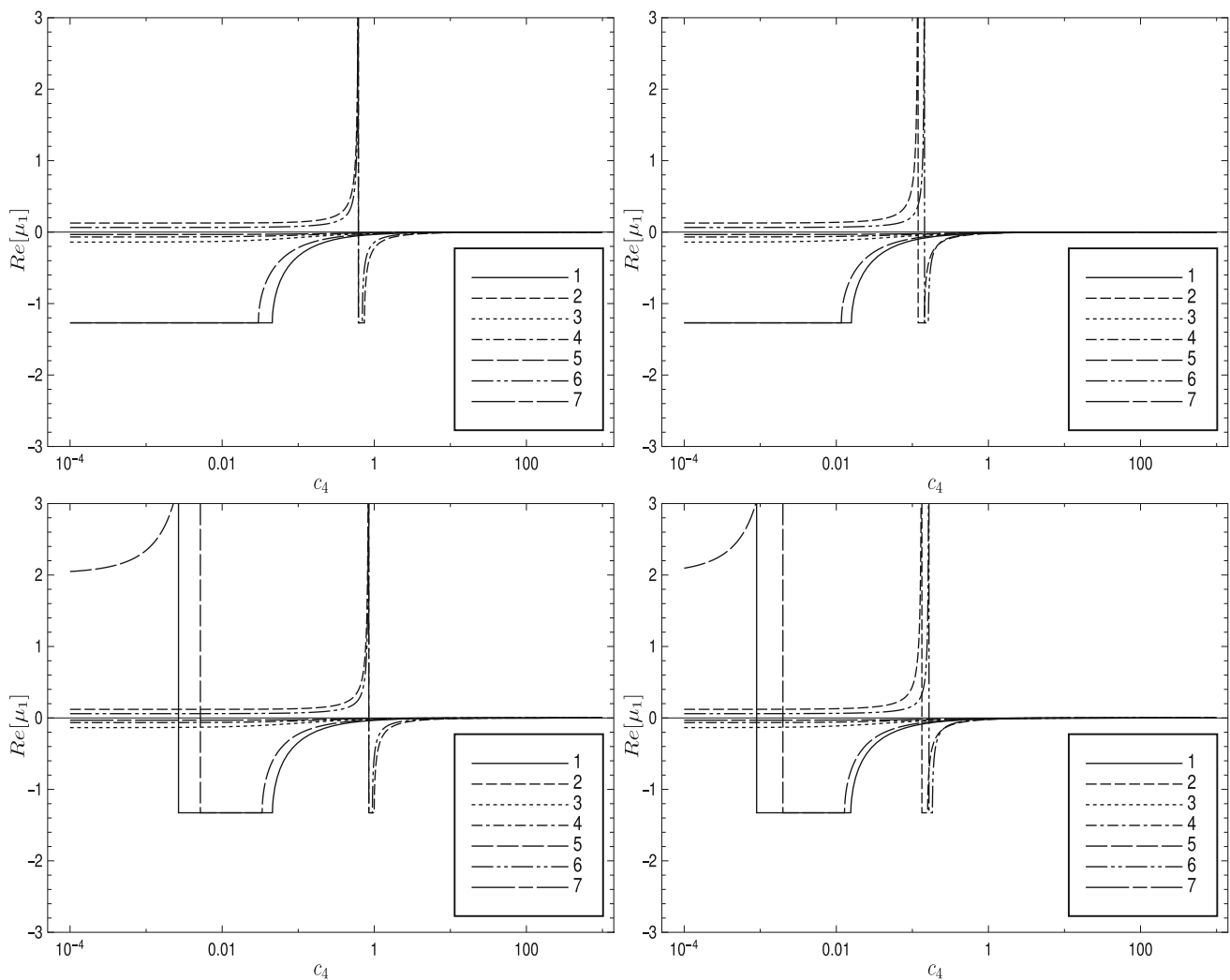
Fig. 1 Plots of the real part of μ_1 as a function of c_4. The upper left, upper right, lower left and lower right panels correspond to $(x_\lambda, n_4) = (0.92, -1), (0.92, -2), (0.69, -1)$ and $(0.69, -2)$, respectively. In the plots, lines 1, 2, 3, 4, 5, 6 and 7 represent the cases of $(n2, n6) = (0, -1), (0, -3), (0, 1), (0, 3), (1, -1), (1, -3)$ and $(1,3)$

matrix are given by

$$E_b = \{\frac{x_\lambda x_{rb} - 6}{2}, x_\lambda x_{rb}(Q_\lambda + 1) - 3\}. \tag{51}$$

It follows from Eq. (50) that observational data require $x_\lambda x_{rb} < 1$ so that the first eigenvalue in Eq. (51) is always negative. We see that if Q_λ does not satisfy Eq. (43), the second eigenvalue in Eq. (51) is negative when $Q_\lambda < 3/(x_\lambda x_{rb}) - 1$ for positive $x_\lambda x_{rb}$ and $Q_\lambda > -3/|x_\lambda x_{rb}| - 1$ for negative $x_\lambda x_{rb}$. These results are the same as those in [47], which implies that the modification of gravity theory has no effect on the stability of the field dominated fixed point. In the case where Q_λ satisfies Eq. (43), one of the eigenvalues vanishes. In this case, the eigenvalues for the field-dominated point are similar to those for the scaling fixed point in which $c_4 \to \infty$. Since one of the eigenvalues vanishes, we cannot

use linear dynamical analysis to estimate the stability of the fixed point. However we will not go beyond the linear analysis in this work. For a given value of x_λ which could make the field-dominated point stable, we can choose n_2, n_4, n_6 and c_4 such that the scaling fixed point is also stable. The question is when the cosmic evolution will reach the scaling fixed point at late time in what situation. Since it is difficult to perform analytical analysis to answer this question, we solve the autonomous equations numerically and plot the evolution of Ω_m in Fig. 2 for some values of the model parameters.

According to Fig. 2, the cosmic evolution will reach the scaling fixed point at late time if $x_r > 0$ during the matter domination. For $x_r < 0$ during the matter domination, the cosmic evolution will evolve toward the field-dominated point. This result is a consequence of a positive x_λ of the scaling points given by Eq. (33), and the fact that the evolu-
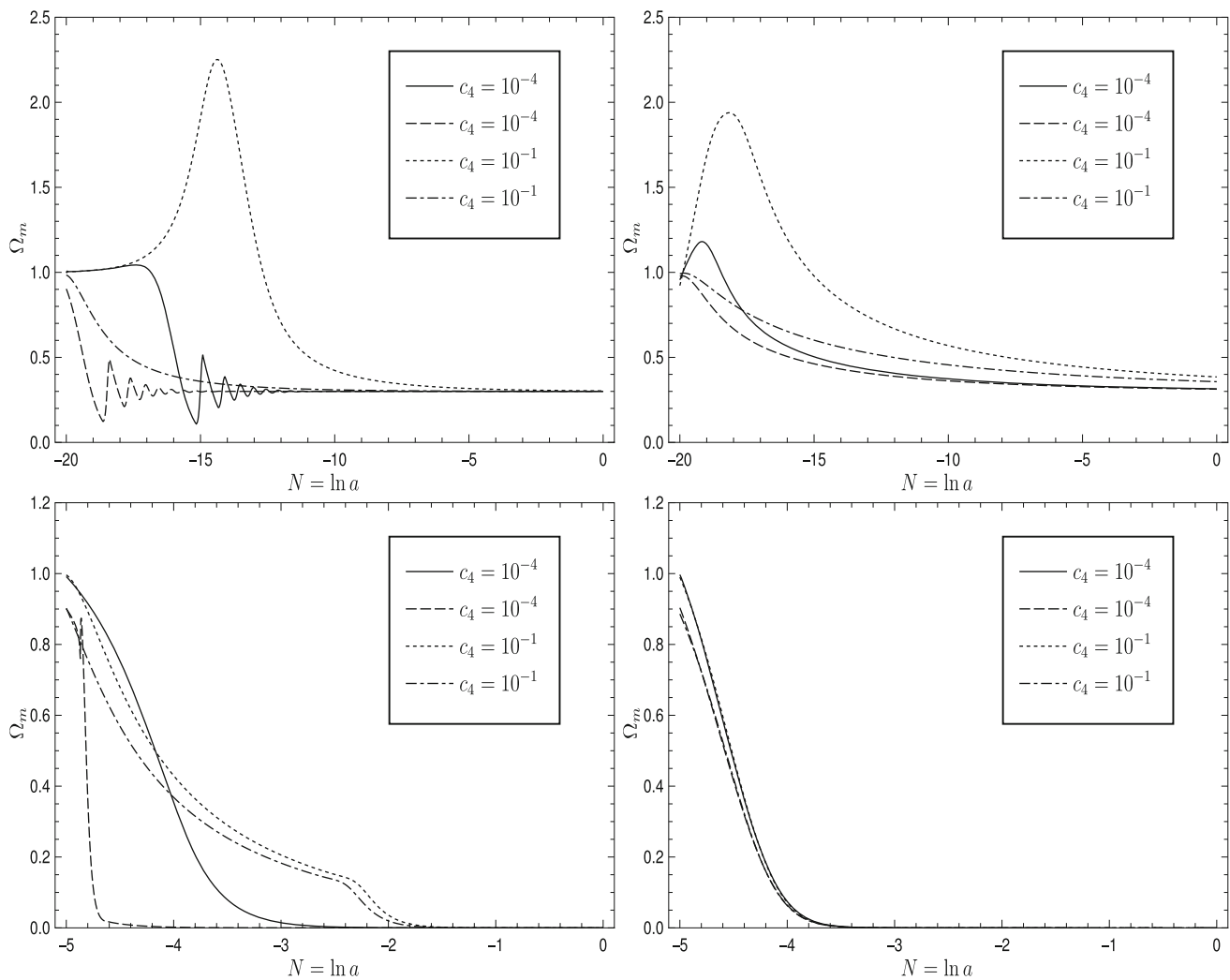
Fig. 2 Plots of Ω_m as a function of N. The upper two panels represent the cases $x_r > 0$ during the matter domination, while the lower two panels represent the cases $x_r < 0$ during the matter domination. The two left panels and the two right panels correspond to the model of $(n_2, n_4, n_6) = (0, -1, -1)$ and $(0, -1, 1)$, respectively

tion of x cannot cross $x = 0$. This implies that although one of the eigenvalues vanishes, the field-dominated point can be stable. Since the scaling points we consider in the plots are stable, these points should be reached for wide ranges of initial conditions. However, if c_4 is large enough and the initial condition for y_r differs significantly from its value at the fixed point, the value of Ω_m can be larger than unity before reaching the fixed point. This implies that Ω_ϕ can be negative, so that the definitions in Eq. (20) may not be interpreted as the energy density and pressure of the dark component. These cases are shown in Fig. 2. In the top left panel of Fig. 2, the initial values for x_r and y_r during the matter domination for the solid, long-dashed, dashed and dash-long-dashed lines are $(x_r, y_r) = (0.55, 10^{-5})$, $(0.05, 0.24)$, $(0.1, 10^{-8})$, and $(0.79, 0.7)$, respectively. In the top right panel of Fig. 2, the initial values for x_r and y_r during the matter domina-

tion for the solid, long-dashed, dashed and dash-long-dashed lines are $(x_r, y_r) = (0.4, 0.2)$, $(0.74, 0.8)$, $(0.18, 0.01)$, and $(0.85, 0.8)$, respectively. For the cases where y_r differs significantly from their values at a fixed point, the maximum value of Ω_m during the cosmic evolution increases when c_4 increases. Since c_4 quantifies the deviation from the Einstein gravity, this suggests that the deviation from the Einstein gravity should not be large, to avoid an unphysical value of Ω_m during the cosmic evolution. Moreover, even though the initial values of x_r and y_r during the matter domination are in the same order of magnitude of the value at the fixed point, the slower cosmic evolution reaches the fixed point for positive initial x_r compared with the negative initial value of x_r.

3.2.3 $y_r = 0$: ϕMDE point

According to Eq. (40), the other fixed point corresponds to $y_r = 0$. It follows from Eq. (35) that $y'_r = 0$ when $y_r = 0$. If we also consider Eq. (34), we see that $x'_r = 0$ when $z_r = 2h/x_\lambda$. Here, h for this fixed point is not necessarily equal to $x_\lambda/2$, because x_λ is evaluated at the scaling fixed point (fixed point a). From the definitions of G_2 and G_4 in Eqs. (27) and (28), as well as the definition of y in Eq. (30), we see that the existence of the fixed point $y_r = 0$ requires $n_2 \le 0, n_6 < 0$ and $n_4 < 0$. Here, we demand that $n_2 \ne n_6$ and $n_4 \ne 0$. Inserting $z_r = 2h/x_\lambda$ and $\Omega_\gamma = 0$ into Eqs. (A1), (A2) and (A3), and then taking the limit $y_r \to 0$, we respectively obtain

$$h|_c = \frac{3 + c_2 x_{rc}^2}{2}, \quad \Omega_{mc} = 1 - \frac{c_2 x_{rc}^2}{3} \quad \text{and}$$
$$x_{rc} = -\frac{Q_\lambda x_\lambda}{c_2}, \tag{52}$$

where the subscript $_c$ denotes evaluation at the ϕMDE point. Substituting the above x_{rc} into the expression for Ω_{mc}, we obtain

$$\Omega_{mc} = 1 - \frac{Q_\lambda^2 x_\lambda^2}{3c_2}. \tag{53}$$

This equation shows that c_2 must be positive; otherwise Ω_{mc} is larger than unity. The eigenvalues for this fixed point are

$$E_c = \left\{ -\frac{3}{2} + \frac{Q_\lambda^2 x_\lambda^2}{2c_2}, 3 + \frac{Q_\lambda(1 + Q_\lambda)x_\lambda^2}{c_2} \right\}. \tag{54}$$

These eigenvalues coincide with those in [47]. The first eigenvalue can be written as $-3\Omega_{mc}/2$, so that it is always negative. The second eigenvalue becomes positive when $Q_\lambda > 0$ or $Q_\lambda < -1$ for positive c_2. Since x_λ is evaluated at the scaling fixed point, it follows from Eq. (43) that $Q_\lambda < 1$ yields $x_\lambda < 0$ corresponding to phantom expansion. We now check how the evolution of the universe can move from this fixed point during matter domination to the scaling fixed point at late time. Let us first consider x_{rc} in Eq. (52). We can use Eq. (43) to write $x_{rc} = (x_\lambda - 3)/c_2$. The scaling fixed point can lead to the acceleration of the universe if $x_\lambda < 2$. Hence, x_{rc} is negative. Since x_{rc} is the value of x_r during matter domination in our consideration, the universe will evolve toward the field-dominated point rather than the scaling fixed point as presented in the previous section. For illustration, we plot the evolution of Ω_m in Fig. 3. For given values of x_λ, Q_λ and Ω_{mc}, the value of c_2 can be computed from Eq. (53). From the values of x_λ, Q_λ and c_2, we can compute x_{rc} from Eq. (52) and compute c_4 from Eq. (36) by setting $\Omega_{ms} = 0.3$. Finally, c_6 can be computed from Eq. (37). The models used in the plots are shown in the Table 1.

From Fig. 3, we see that Ω_m evolves toward the field-dominated point for various values of Q_λ which correspond
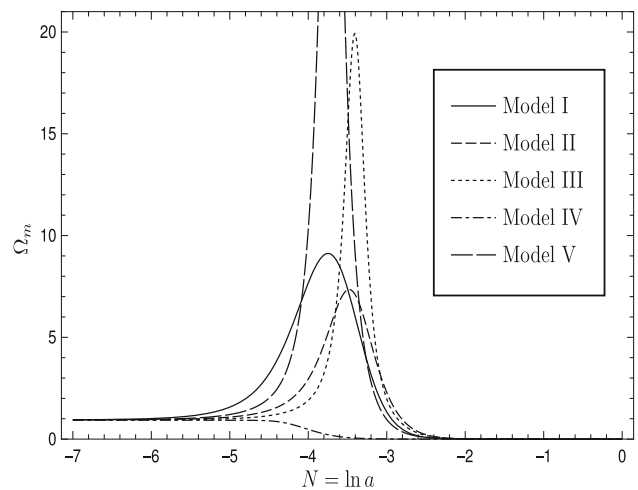
Fig. 3 Plots of Ω_m as a function of N for models I–V given in the table

to various w_{eff} at late time. In the plots, we initially set $y_r = 10^{-11}$ according to the ϕMDE point, so that the value of Ω_m can be larger than unity before reaching the field-dominated point. However, if c_4 is sufficiently small, e.g., $c_4 = 5.6 \times 10^{-3}$ for model IV, Ω_m can be less than unity throughout the evolution of the universe. By definition, c_4 quantifies the size of the deviation from the Einstein gravity. The above results suggest that the deviation from the Einstein gravity should not be large, to avoid the case $\Omega_m > 1$ during the cosmic evolution. From the analysis of the Vainshtein mechanism, the bound on the difference between the gravitational constant of the gravitational source and the gravitational coupling for GW gives [36]

$$\left| \frac{XG_{4X}}{G_4} \right| < \mathcal{O}(10^{-3}). \tag{55}$$

In terms of c_4, $|XG_{4X}| = |n_4 c_4|$ at the scaling fixed point. Hence, the small c_4 seems to agree with the above bound.

4 Stability of the linear perturbations

In this section, we investigate the stability of the linear perturbations in the theory considered in the previous sections around the FLRW background. To describe the perturbations in the metric tensor, we use the metric tensor in the ADM form,

$$ds^2 = -n^2 dt^2 + h_{ij}(dx^i + n^i dt)(dx^j + n^j dt), \tag{56}$$

and quantify the scalar perturbations in the unitary gauge by field variables δn, ψ and ζ as

$$n = 1 + \delta n, \quad n^i = \delta^{ij} \partial_j \psi, \quad h_{ij} = e^{2\zeta} \delta_{ij}. \tag{57}$$

Table 1 The models used in the plots. We set $\Omega_{m\,c} = 0.95$ for models I–IV and $\Omega_{m\,c} = 0.93$ for model V. The column w_{eff} shows the value of w_{eff} at the field-dominated point

Model	(n_2, n_4, n_6)	Q_λ	x_{rc}	c_4	w_{eff}
I	$(0, -1, -1)$	-10	-0.045	7.7	-0.88
II	$(0, -1, -1)$	2	-0.075	1.7	-1.28
III	$(0, -1, -1)$	$2/3$	-0.125	0.67	-1.44
IV	$(0, -1, -1)$	$1/6$	-0.49	5.6×10^{-3}	-1.47
V	$(0, -1, -2)$	2	-0.075	4.0	-1.17

The perturbed action for the DHOST theories up to the second order in perturbation is [50]

$$S^{(2)} = \int \mathrm{d}^3x \, \mathrm{d}t \, a^3 \frac{M^2}{2} \left[A_{\tilde{\zeta}} \dot{\tilde{\zeta}}^2 - B_{\tilde{\zeta}} \frac{(\partial_i \tilde{\zeta})^2}{a^2} + C_{\tilde{\zeta}} \frac{(\partial_i \dot{\tilde{\zeta}})^2}{a^2} \right],$$
(58)

where the propagating scalar degree of freedom is described by

$$\tilde{\zeta} \equiv \zeta - \beta_1 \delta n.$$
(59)

The coefficients in the action (58) are given by

$$A_{\tilde{\zeta}} = \frac{1}{(1 + \alpha_B - \dot{\beta}_1/H)^2} \alpha,$$
(60)

$$B_{\tilde{\zeta}} = -2(1 + \alpha_T) + \frac{2}{aM^2} \frac{\mathrm{d}}{\mathrm{d}t} \left[\frac{aM^2 \left(1 + \alpha_H + \beta_1 (1 + \alpha_T) \right)}{H(1 + \alpha_B) - \dot{\beta}_1} \right],$$
(61)

$$C_{\tilde{\zeta}} = \frac{4(1 + \alpha_H)\beta_1 + 2(1 + \alpha_T)\beta_1^2 + \beta_3}{(1 + \alpha_B - \dot{\beta}_1/H)^2}.$$
(62)

Here,

$$\alpha \equiv \alpha_K + 6\alpha_B^2 - \frac{6}{a^3 H^2 M^2} \frac{d}{dt} \left(a^3 H M^2 \alpha_B \beta_1 \right).$$
(63)

For the action in Eq. (10), the variables M^2, α_K, α_B, α_H, α_L, α_T, β_1, β_2 and β_3 defined in [11,50] are

$$M^2 = 2G_4, \quad \alpha_T = 0, \quad \alpha_L = 0,$$
(64)

$$\alpha_B = 2\beta_1 + \frac{\dot{\phi} \left(6G_{4X}\ddot{\phi} + 2XG_{4\phi X} + G_{4\phi} \right)}{2G_4 H},$$

$$\frac{4HXG_{4X} + \dot{\phi} \left(6G_{4X}\ddot{\phi} + 2XG_{4\phi X} + G_{4\phi} \right)}{2G_4 H},$$
(65)

$$\alpha_H = -2\beta_1, \quad \beta_1 = \frac{XG_{4X}}{G_4}, \quad \beta_2 = -3\beta_1^2,$$

$$\beta_3 = 6\beta_1^2 - 4\beta_1,$$
(66)

and

$$\alpha_K = \frac{2X \left(G_{2X} + 2XG_{2XX} \right)}{G_4 H^2}$$

$$- \frac{6X \left(H \left(G_{4X} + 2XG_{4XX} \right) + \dot{\phi} \left(2XG_{4\phi XX} + 3G_{4\phi X} \right) \right)}{G_4 H}$$

$$- \frac{36\ddot{\phi}}{\dot{\phi} H} \beta_1 - \frac{6\ddot{\phi}^2}{XH^2}$$

$$\left(4\beta_1^4 - \left(13\beta_1 + 10X^2 \frac{G_{4XX}}{G_4} \right) \beta_1^2 \right.$$

$$+ 15\beta_1^2 + 2X^2 \left(13 \frac{G_{4XX}}{G_4} + 2X \frac{G_{4XXX}}{G_4} \right) \beta_1$$

$$\left. + 4 \left(X^2 \frac{G_{4XX}}{G_4} \right)^2 \right).$$
(67)

According to Eqs. (58) and (63), the no-ghost condition is

$$\alpha > 0.$$
(68)

We now add matter into our consideration by supposing that the matter is described by K-essence [30,50] for which the action is

$$S_m = \int \mathrm{d}^4x \sqrt{-\tilde{g}} P(Y), \quad Y \equiv -\tilde{g}^{\mu\nu} \partial_\mu \sigma \, \partial_\nu \sigma,$$
(69)

where σ is the scalar field, and the metric $\tilde{g}_{\mu\nu}$ is related to the metric $g_{\mu\nu}$ in the action (10) by the conformal transformation,

$$\tilde{g}_{\mu\nu} = \mathrm{e}^{2Q\phi} g_{\mu\nu}.$$
(70)

It can be shown that the action for the matter in the form of Eq. (69) can lead to Eq. (19) (see, e.g., [55,56]). Including the matter, the action (58) becomes [31,50]

$$S = \int \mathrm{d}^3x \, \mathrm{d}t \, a^3 \frac{M^2}{2} \left\{ \dot{\mathcal{V}} \mathcal{K} \dot{\mathcal{V}}^T - \frac{1}{a^2} \partial_i \mathcal{V} \mathcal{L} \partial^i \mathcal{V}^T, \right\},$$
(71)

where $\mathcal{V} \equiv (\tilde{\zeta}, \delta\sigma)$, and $\delta\sigma$ describes the perturbations in the field σ. The matrix $\mathcal{K}$ and $\mathcal{L}$ are defined as

$$\mathcal{K} \equiv \begin{pmatrix} \tilde{A}_{\tilde{\zeta}} & B_m \\ B_m & A_m \end{pmatrix}, \quad \mathcal{L} \equiv \begin{pmatrix} B_{\tilde{\zeta}} & C_m \\ C_m & A_m c_m^2 \end{pmatrix},$$
(72)

where $c_m^2 \equiv P_Y/(P_Y + 2Y P_{YY})$ is the square of the sound speed of the matter perturbations, a subscript $_Y$ denotes derivative with respect to Y, and

$$A_m \equiv \frac{2\mathrm{e}^{2Q\phi} P_Y}{M^2 c_m^2},$$
(73)

$$\tilde{A}_{\tilde{\zeta}} = A_{\tilde{\zeta}} + \frac{\mathcal{M}}{\left[H(1 + \alpha_B) - \dot{\beta}_1 \right]^2},$$
(74)

$$B_m = \frac{e^{2Q\phi}\rho_m(1+w_m)}{\dot{\sigma}_0 M^2 c_m^2} \frac{1-3c_m^2\beta_1}{H(1+\alpha_{\rm B})-\dot{\beta}_1},$$ (75)

$$C_m = \frac{e^{2Q\phi}\rho_m(1+w_m)}{\dot{\sigma}_0 M^2} \frac{1+\alpha_{\rm H}+\beta_1(1+\alpha_{\rm T})}{H(1+\alpha_{\rm B})-\dot{\beta}_1},$$ (76)

The quantity $\dot{\sigma}_0$ is the time derivative of the background field σ_0 and

$$\mathcal{M} = 3\hat{\Omega}_m H^2 \left[(1+w_m)\left(6\beta_1 - 9c_m^2\beta_1^2\right) + 6w_m\beta_1 \right]$$
$$+ \frac{e^{2Q\phi}\rho_m(1+w_m)}{c_m^2 M^2}\left[1-3c_m^2\beta_1\right]^2,$$ (77)

$$\hat{\Omega}_m = \frac{e^{4Q\phi}(2YP_Y-P)}{3M^2H^2}.$$ (78)

The ghost and gradient instabilities can be avoided if the eigenvalues of the matrices $\mathcal{K}$ and $\mathcal{L}$ are positive. From Eq. (72), the eigenvalues of these matrices can be written in the forms

$$\lambda_{\mathcal{K}} = \frac{1}{2}\left((\tilde{A}_{\tilde{\zeta}}+A_m) \pm \sqrt{(\tilde{A}_{\tilde{\zeta}}+A_m)^2 - 4(\tilde{A}_{\tilde{\zeta}}A_m - B_m^2)} \right),$$ (79)

$$\lambda_{\mathcal{L}} = \frac{1}{2}\left((B_{\tilde{\zeta}}+A_m c_m^2) \right.$$
$$\left. \pm \sqrt{(B_{\tilde{\zeta}}+A_m c_m^2)^2 - 4(B_{\tilde{\zeta}}A_m c_m^2 - C_m^2)} \right).$$ (80)

We see that the model can be free from ghost instability if $\tilde{A}_{\tilde{\zeta}} > 0$, $A_m > 0$ and $\tilde{A}_{\tilde{\zeta}}A_m > B_m^2$. Since A_m is the coefficient of the kinetic term for the matter, we expect that $A_m > 0$. The coefficient $\tilde{A}_{\tilde{\zeta}} > 0$ if Eq. (68) is satisfied. Using the limit $w_m \to 0$ and $c_e^2 \to 0$, the condition $\tilde{A}_{\tilde{\zeta}}A_m > B_m^2$ can be satisfied. Hence, even though the matter is included in the consideration, the no-ghost condition is still given by Eq. (68). Similar to the case of ghost instability, the model can be free from gradient instability if $B_{\tilde{\zeta}} > 0$, $A_m c_m^2 > 0$ and $B_{\tilde{\zeta}}A_m c_m^2 > C_m^2$. To check the latter condition, we write

$$B_{\tilde{\zeta}}A_m c_m^2 - C_m^2$$
$$= \frac{2e^{2Q\phi}P_Y}{M^2}\left[B_{\tilde{\zeta}} - \frac{3e^{2Q\phi}\Omega_m}{M^2}\left[\frac{1+\alpha_{\rm H}+\beta_1}{(1+\alpha_{\rm B})-\beta_1'}\right]^2 \right]$$
$$= \frac{2e^{2Q\phi}P_Y}{M^2}\mathcal{C}.$$ (81)

Hence, the gradient instability can be avoided if $B_{\tilde{\zeta}} > 0$ and $\mathcal{C} > 0$. We now estimate the factor $e^{2Q\phi}$ in the expression for $\mathcal{C}$. It is difficult to estimate the value of ϕ from the results in the previous sections, so we estimate Q from Eq. (43), which gives $Q/\lambda \simeq 2.2$ if $x_\lambda \simeq 0.92$. Since the background dynamics discussed in the previous sections depend on Q/λ rather than Q, for a given value of Q/λ, we can choose λ such that Q is small or negative without altering the background dynamics. Hence, for simplicity, we suppose that $e^{2Q\phi} \lesssim 1$.

We check the ghost and gradient instabilities at the scaling point which corresponds to the cosmic acceleration at late time. We choose $x_\lambda \simeq 0.92$, $\Omega_m = 0.3$ and $c_4 = 0.1$. We write α, $B_{\tilde{\zeta}}$ and $\mathcal{C}$ in terms of dimensionless variables and compute numerical values of these quantities. We have found that there is no gradient instability, and the ghost instability can be avoided if $n_6 > n_2$ for $n_2 \geq 0$ and for a wide range of n_4. These conclusions do not depend on c_4.

5 Conclusions

In this work, we have studied the cosmic evolution based on the fixed points in the dynamical analysis of the DHOST theory which has scaling solutions. In addition to the scaling solutions, the DHOST theory in our consideration satisfies the requirements that the propagation speed of GW is equal to the speed of light and the GW do not decay to dark energy perturbations. We concentrate on the model parameters for which the expression of z_r is given by Eq. (A5).

We have found in our analysis that the scaling fixed point associated with the late-time accelerating universe is stable when n_2 and n_6 are not negative for $n_4 = -1$ and -2. The stability of this scaling fixed point also depends on the expansion rate of the universe at late time through the parameter x_λ. There are ranges of parameters in which the scaling fixed point and the field-dominated point are simultaneously stable. The cosmic evolution will reach the scaling fixed point at late time if x_r when the matter domination is positive. If x_r during the matter domination is negative, the cosmic evolution will reach the field-dominated point.

When the scaling fixed point and the field-dominated point are stable, these points can be reached at late time for wide ranges of x_r and y_r during the matter domination. However, we have found that the density parameter of the matter can be larger than unity during the cosmic evolution if c_4 is large enough and the initial value of y_r during the matter domination is significantly different from its value at those fixed points. By definition, c_4 quantifies the size of the deviation from the Einstein gravity. In our consideration, the allowed values of c_4 depend on the initial conditions for x_r and y_r during the matter domination.

Even though the autonomous equations for the model considered here are different from coupled dark energy models presented in [47], we have found that the eigenvalues for the field-dominated and ϕMDE points in both models are the same. In our numerical investigation, the universe can only evolve from the ϕMDE to the field-dominated point. We have also found that the eigenvalues for the scaling fixed point reduce to those for the field-dominated point when c_4 is significantly large. However, recall that the large c_4 can lead to unphysical values of Ω_m during the cosmic evolution.

We conclude that the fixed points for the DHOST theory studied in [49] are similar to those in the coupled dark energy model in [47]. We have found that the eigenvalues for the field-dominated and ϕMDE points in DHOST theory with scaling solutions are similar to those in the coupled dark energy model even though the theories of gravity in these models are different. However, for DHOST theory, the expressions for the eigenvalues corresponding to the scaling point are complicated, and consequently the stability of the fixed point is evaluated numerically in this work.

We have also estimated the ghost and gradient instabilities in this theory. We have found that this theory is free from the gradient instability, while the ghost instability is absent when $n_6 > n_2$ for $n_2 \geq 0$ and for a wide range of n_4.

Data Availability Statement This manuscript has no associated data or the data will not be deposited. [Authors' comment: This manuscript does not use any data in the analysis.]

Appendix A: Constraint equations in terms of dimensionless variables

In terms of the dimensionless variables, we can write Eq. (15) as

$$
\begin{aligned}
0 = \frac{1}{2c_4 + v_r^{n_4}} \Big[& v_r^{-n_4} \left(v_r^{-n_2-n_6} \left(2c_4 + v_r^{n_4} \right) \left(2c_4 n_4 v_r^{n_2+n_6} \right. \right. \\
& \left(z_r x_\lambda \left(-\frac{\dot{H}}{H^2} + z_r x_\lambda - 2 \right) - x_\lambda z_r' + n_4 x_\lambda^2 \right) \\
& \left. -x_r^2 v_r^{n_4} \left(c_6 v_r^{n_2} - c_2 v_r^{n_6} \right) \right) + \left(2c_4 + v_r^{n_4} \right) \left(c_4 \left(4\frac{\dot{H}}{H^2} + 6 \right) \right. \\
& \left. \left. + \left(2\frac{\dot{H}}{H^2} + \Omega_\gamma + 3 \right) v_r^{n_4} \right) \right) \\
& + c_4 n_4 z_r^2 x_\lambda^2 \left(c_4 \left(n_4 - 4 \right) \right. \\
& + 2 \left(n_4 - 1 \right) v_r^{n_4} \right) - 4c_4 n_4^2 z_r x_\lambda^2 \left(2c_4 + v_r^{n_4} \right) \\
& \left. - c_4 n_4 x_\lambda \left(2c_4 + v_r^{n_4} \right) \left(z_r x_\lambda - 4 \right) \right], \qquad (A1)
\end{aligned}
$$

where $v_r \equiv y_r / x_r^2$.

Equation (16) can be written in terms of the dimensionless variables as

$$
\begin{aligned}
0 = \frac{1}{\left(2c_4 + v_r^{n_4} \right)^2} \big[& v_r^{-n_2-n_4-n_6} (-c_4^2 v_r^{n_4} \\
& (-4c_6 \left(3n_4 - 2n_6 - 1 \right) x_r^2 v_r^{n_2} - 4c_2 \left(2n_2 - 3n_4 + 1 \right) x_r^2 v_r^{n_6} \\
& + 3v_r^{n_2+n_6} (4n_4^3 x_r^2 x_\lambda^2 + 4n_4 (2x_r x_\lambda \\
& - 2z_r x_\lambda + \Omega_\gamma - 2) + n_4^2 x_\lambda (x_r \left(8 - 2z_r x_\lambda \right) \\
& + z_r \left(z_r x_\lambda + 4 \right)) + 12)) - 2c_4 v_r^{2n_4} \\
& (-c_6 \left(3n_4 - 4n_6 - 2 \right) x_r^2 v_r^{n_2} - c_2 \left(4n_2 - 3n_4 + 2 \right) x_r^2 v_r^{n_6} \\
& + 3v_r^{n_2+n_6} \left(n_4 \left(x_r x_\lambda - z_r x_\lambda + \Omega_\gamma - 1 \right) + 3 \right)) \\
& - 6c_4^3 v_r^{n_2+n_6} (n_4^3 x_\lambda^2 \left(-4x_r z_r + 4x_r^2 - z_r^2 \right) \\
& + n_4^2 x_\lambda (x_r \left(8 - 2z_r x_\lambda \right) \\
& + z_r \left(z_r x_\lambda + 4 \right)) + 4n_4 \left(x_\lambda \left(x_r - z_r \right) - 1 \right) + 4) \\
& + v_r^{3n_4} (-c_6 \left(2n_6 + 1 \right) x_r^2 v_r^{n_2} + c_2 \left(2n_2 + 1 \right) x_r^2 v_r^{n_6} \\
& - 3v_r^{n_2+n_6}))] + 3 \left(\Omega_m + \Omega_\gamma \right). \qquad (A2)
\end{aligned}
$$

This equation can be used to express Ω_m in terms of the other dimensionless variables. Equation (22) can be written in terms of the dimensionless variables as

$$
\begin{aligned}
0 = v_r^{-n_2-4n_4-n_6} \big(c_4^3 \big(& -6n_4^4 \\
& (8x_r^3 - 18z_r x_r^2 + 9z_r^2 x_r + z_r^3) x_\lambda^3 v_r^{n_2+n_6} \\
& + 3n_4^3 x_\lambda^2 \left(8x_\lambda x_r^3 - 96x_r^2 - 3z_r \right. \\
& \left. (z_r x_\lambda - 24) x_r + z_r^2 \left(z_r x_\lambda + 12 \right) \right) v_r^{n_2+n_6} \\
& + 12n_4 \left(c_6 x_r^2 ((2n_6 - 1) x_r x_\lambda - (2n_6 z_r + z_r) x_\lambda + 8) v_r^{n_2} \right. \\
& - c_2 x_r^2 ((2n_2 - 1) x_r x_\lambda \\
& - (2n_2 z_r + z_r) x_\lambda + 8) v_r^{n_6} + (x_r - z_r) \left(\Omega_\gamma - 3 \right) x_\lambda v_r^{n_2+n_6}) \\
& - 12n_4^2 x_\lambda \left(c_6 x_r^2 \right. \\
& (2x_r + z_r) v_r^{n_2} \\
& - c_2 x_r^2 \left(2x_r + z_r \right) v_r^{n_6} + (x_\lambda \left(z_r x_\lambda - 4 \right) \\
& x_r^2 - 2 \left(\Omega_\gamma + 2z_r x_\lambda - 7 \right) x_r \\
& + z_r \left(-\Omega_\gamma + 2z_r x_\lambda + 4 \right)) v_r^{n_2+n_6}) + 8x_r \left(3v_r^{n_2+n_6} \right. \\
& \left(\Omega_m + \Omega_\gamma \right) Q_\lambda x_\lambda \\
& - x_r \left(c_6 v_r^{n_2} \left(2 \left(x_r - z_r \right) x_\lambda n_6^2 + (x_r x_\lambda - 3z_r x_\lambda + 6) n_6 - z_r x_\lambda + 6 \right) \right. \\
& - c_2 v_r^{n_6} \left(2 \left(x_r - z_r \right) x_\lambda n_2^2 \right. \\
& \left. + (x_r x_\lambda - 3z_r x_\lambda + 6) n_2 - z_r x_\lambda + 6)))) \\
& v_r^{n_4} - 3c_4^2 \left(8n_4^4 x_r^2 \left(x_r - z_r \right) x_\lambda^3 v_r^{n_2+n_6} \right. \\
& - 2n_4^3 x_\lambda^2 \left(x_\lambda x_r^3 + (z_r x_\lambda - 16) x_r^2 + 8z_r x_r + 2z_r^2 \right) v_r^{n_2+n_6} \\
& + n_4 \left(-4c_6 x_r^2 ((2n_6 - 1) x_r x_\lambda \right. \\
& - (2n_6 z_r + z_r) x_\lambda + 8) v_r^{n_2} + 4c_2 x_r^2 ((2n_2 - 1) x_r x_\lambda \\
& - (2n_2 z_r + z_r) x_\lambda + 8) v_r^{n_6} \\
& - 2 \left(x_r - z_r \right) \left(2\Omega_\gamma - 3 \right) x_\lambda v_r^{n_2+n_6}) \\
& + n_4^2 x_\lambda \left(6c_6 x_r^2 z_r v_r^{n_2} - 6c_2 x_r^2 z_r v_r^{n_6} + \left(x_\lambda \left(z_r x_\lambda - 4 \right) x_r^2 \right. \right. \\
& + (8 - 4z_r x_\lambda) x_r + 2z_r \left(-3\Omega_\gamma + z_r x_\lambda + 5 \right)) v_r^{n_2+n_6}) \\
& - 4x_r \left(3v_r^{n_2+n_6} \left(\Omega_m + \Omega_\gamma \right) Q_\lambda x_\lambda \right. \\
& - x_r \left(c_6 v_r^{n_2} \left(2 \left(x_r - z_r \right) x_\lambda n_6^2 + (x_r x_\lambda - 3z_r x_\lambda + 6) n_6 - z_r x_\lambda + 6 \right) \right. \\
& - c_2 v_r^{n_6} \left(2 \left(x_r - z_r \right) x_\lambda n_2^2 \right. \\
& \left. + (x_r x_\lambda - 3z_r x_\lambda + 6) n_2 - z_r x_\lambda + 6)))) v_r^{2n_4}
\end{aligned}
$$

$$
\begin{aligned}
&-3c_4 \left(2\left(x_r-z_r\right)\left(-c_6 x_r^2 v_r^{n_2}+c_2 x_r^2 v_r^{n_6}+\left(\Omega_\gamma-1\right) v_r^{n_2+n_6}\right) x_\lambda n_4^2\right.\\
&+\left(-c_6 x_r^2\left(\left(2n_6-1\right) x_r x_\lambda\right.\right.\\
&\quad -\left(2n_6 z_r+z_r\right) x_\lambda+8\right) v_r^{n_2}+c_2 x_r^2\left(\left(2n_2-1\right) x_r x_\lambda\\
&\quad -\left(2n_2 z_r+z_r\right) x_\lambda+8\right) v_r^{n_6}\\
&\quad -\left(x_r-z_r\right)\left(\Omega_\gamma-1\right) x_\lambda v_r^{n_2+n_6}\right) n_4-2x_r\left(3 v_r^{n_2+n_6}\right.\\
&\left(\Omega_m+\Omega_\gamma\right) Q_\lambda x_\lambda\\
&-x_r\left(c_6 v_r^{n_2}\left(2\left(x_r-z_r\right) x_\lambda n_6^2+\left(x_r x_\lambda-3z_r x_\lambda+6\right) n_6-z_r x_\lambda+6\right)\right.\\
&-c_2 v_r^{n_6}\left(2\left(x_r-z_r\right) x_\lambda n_2^2\right.\\
&\left.\left.\left.+\left(x_r x_\lambda-3z_r x_\lambda+6\right) n_2-z_r x_\lambda+6\right)\right)\right) v_r^{3n_4}+x_r\left(3 v_r^{n_2+n_6}\right.\\
&\left(\Omega_m+\Omega_\gamma\right) Q_\lambda x_\lambda\\
&-x_r\left(c_6 v_r^{n_2}\left(2\left(x_r-z_r\right) x_\lambda n_6^2+\left(x_r x_\lambda-3z_r x_\lambda+6\right) n_6-z_r x_\lambda+6\right)\right.\\
&-c_2 v_r^{n_6}\left(2\left(x_r-z_r\right) x_\lambda n_2^2\right.\\
&\left.\left.\left.+\left(x_r x_\lambda-3z_r x_\lambda+6\right) n_2-z_r x_\lambda+6\right)\right)\right) v_r^{4n_4}\\
&+6c_4^4 n_4 x_\lambda\left(4n_4^2 x_\lambda^2 x_r^3+2n_4 x_\lambda\left(2z_r x_\lambda n_4^2-2\left(z_r x_\lambda+8\right) n_4-z_r x_\lambda+4\right) x_r^2\right.\\
&-\left(12z_r^2 x_\lambda^2 n_4^3+z_r x_\lambda\left(3z_r x_\lambda-40\right) n_4^2-8\left(z_r x_\lambda-4\right) n_4+4\right) x_r\\
&\left.\left.-\left(n_4-1\right) z_r\left(n_4 z_r x_\lambda-2\right)^2\right) v_r^{n_2+n_6}\right).
\end{aligned}
\tag{A3}
$$

To compute the equation for z_r, we substitute Ω_m solved from Eq. (A2) into the above equation. The resulting equation can be written in the form

$$
b_3 z_r^3+b_2 z_r^2+b1 z_r+b_0=0\,,
\tag{A4}
$$

where b_0, b_1, b_2 and b_3 are complicated functions of the dimensionless variables of Ω_γ, x_r, y_r and x_λ. Using Eq. (A4), we can compute the expression for z_r in the form

$$
z_{r\,1}=-\frac{\sqrt[3]{2}\left(3b_1 b_3-b_2^2\right)}{3b_3 \sqrt[3]{\Delta}}+\frac{\sqrt[3]{\Delta}}{3\sqrt[3]{2}b_3}-\frac{b_2}{3b_3},
\tag{A5}
$$

$$
z_{r\,2}=\frac{\left(1+i\sqrt{3}\right)\left(3b_1 b_3-b_2^2\right)}{3(2^{2/3}b_3 \sqrt[3]{\Delta})}-\frac{\left(1-i\sqrt{3}\right)\sqrt[3]{\Delta}}{6\sqrt[3]{2}b_3}-\frac{b_2}{3b_3},
\tag{A6}
$$

$$
\begin{aligned}
z_{r\,3}=&\frac{\left(1-i\sqrt{3}\right)\left(3b_1 b_3-b_2^2\right)}{3(2^{2/3}b_3 \sqrt[3]{\Delta})}\\
&-\frac{\left(1+i\sqrt{3}\right)\sqrt[3]{\Delta}}{6\sqrt[3]{2}b_3}-\frac{b_2}{3b_3},
\end{aligned}
\tag{A7}
$$

where $\Delta=-2b_2^3+9b_1 b_3 b_2-27b_0 b_3^2+\sqrt{4\left(3b_1 b_3-b_2^2\right)^3+\left(-2b_2^3+9b_1 b_3 b_2-27b_0 b_3^2\right)^2}$.
The physically relevant solution is selected from the above solutions by the requirement that z_r becomes unity when $x_r=y_r=1$, $\Omega_\gamma=0$, and c_2 and c_6 are given by Eqs. (36) and (37).

References

1. Supernova Search Team Collaboration, A. Riess et al., Astron. J. **116**, 1009–1038 (1998). arXiv:astro-ph/9805201
2. Supernova Cosmology Project Collaboration, S. Perlmutter et al., Astrophys. J. **517**, 565–586 (1999). arXiv:astro-ph/9812133
3. T. Clifton, P.G. Ferreira, A. Padilla, C. Skordis, Phys. Rep. **513**, 1–189 (2012). [arXiv:1106.2476 [astro-ph.CO]]
4. C. Brans, R.H. Dicke, Phys. Rev. **124**, 925–935 (1961)
5. G.W. Horndeski, Int. J. Theor. Phys. **10**, 363–384 (1974)
6. Y. Fujii, K. Maeda, (Cambridge University Press, 2003)
7. C. Deffayet, X. Gao, D.A. Steer, G. Zahariade, Phys. Rev. D **84**, 064039 (2011). arXiv:1103.3260 [hep-th]
8. C. Charmousis, E.J. Copeland, A. Padilla, P.M. Saffin, Phys. Rev. Lett. **108**, 051101 (2012). arXiv:1106.2000 [hep-th]
9. J. Gleyzes, D. Langlois, F. Piazza, F. Vernizzi, JCAP **08**, 025 (2013). arXiv:1304.4840 [hep-th]
10. C. Lin, S. Mukohyama, R. Namba, R. Saitou, JCAP **10**, 071 (2014). arXiv:1408.0670 [hep-th]
11. J. Gleyzes, D. Langlois, F. Piazza, F. Vernizzi, JCAP **02**, 018 (2015). arXiv:1408.1952 [astro-ph.CO]
12. D. Langlois, K. Noui, JCAP **02**, 034 (2016). arXiv:1510.06930 [gr-qc]
13. M. Crisostomi, K. Koyama, G. Tasinato, JCAP **04**, 044 (2016). arXiv:1602.03119 [hep-th]
14. J. Ben Achour, D. Langlois, K. Noui, Phys. Rev. D **93**, 124005 (2016). arXiv:1602.08398 [gr-qc]
15. J.B. Achour, M. Crisostomi, K. Koyama, D. Langlois, K. Noui, JHEP **12**, 100 (2016). arXiv:1608.08135 [hep-th]
16. M. Crisostomi, M. Hull, K. Koyama, G. Tasinato, JCAP **03**, 038 (2016). arXiv:1601.04658 [hep-th]
17. B.P. Abbott et al., Astrophys. J. Lett. **848**, L13 (2017). arXiv:1710.05834 [astro-ph.HE]
18. B.P. Abbott et al., Phys. Rev. Lett. **119**, 161101 (2017). arXiv:1710.05832 [gr-qc]
19. D.A. Coulter et al., Science **35**, 1556 (2017). arXiv:1710.05452 [astro-ph.HE]
20. B.P. Abbott et al., Astrophys. J. Lett. **848**, L12 (2017). arXiv:1710.05833 [astro-ph.HE]
21. A. Murguia-Berthier et al., Astrophys. J. Lett. **848**, L34 (2017). arXiv:1710.05453 [astro-ph.HE]
22. L. Lombriser, A. Taylor, JCAP **03**, 031 (2016). arXiv:1509.08458 [astro-ph.CO]
23. L. Lombriser, N.A. Lima, Phys. Lett. B **765**, 382 (2017). arXiv:1602.07670 [astro-ph.CO]
24. D. Bettoni, J.M. Ezquiaga, K. Hinterbichler, M. Zumalacárregui, Phys. Rev. D **95**, 084029 (2017). arXiv:1608.01982 [gr-qc]
25. P. Creminelli, F. Vernizzi, Phys. Rev. Lett. **119**, 251302 (2017). arXiv:1710.05877 [astro-ph.CO]
26. J. Sakstein, B. Jain, Phys. Rev. Lett. **119**, 251303 (2017). arXiv:1710.05893 [astro-ph.CO]
27. J.M. Ezquiaga, M. Zumalacárregui, Phys. Rev. Lett. **119**, 251304 (2017). arXiv:1710.05901 [astro-ph.CO]
28. T. Baker, E. Bellini, P.G. Ferreira, M. Lagos, J. Noller, I. Sawicki, Phys. Rev. Lett. **119**, 251301 (2017). arXiv:1710.06394 [astro-ph.CO]
29. S. Arai, A. Nishizawa, Phys. Rev. D **97**, 104038 (2018). arXiv:1711.03776 [gr-qc]
30. R. Kase, S. Tsujikawa, Phys. Rev. D **97**, 103501 (2018). arXiv:1802.02728 [gr-qc]
31. M. Crisostomi, K. Koyama, D. Langlois, K. Noui, JCAP **01**, 030 (2019). arXiv:1810.12070 [hep-th]
32. S. Hirano, T. Kobayashi, D. Yamauchi, S. Yokoyama, Phys. Rev. D **99**, 104051 (2019). arXiv:1902.02946 [astro-ph.CO]
33. H. Boumaza, D. Langlois, K. Noui, Phys. Rev. D **102**, 024018 (2020). arXiv:2004.10260 [astro-ph.CO]
34. D. Langlois, K. Noui, H. Roussille, Phys. Rev. D **103**, 084022 (2021). arXiv:2012.10218 [gr-qc]
35. P. Creminelli, M. Lewandowski, G. Tambalo, F. Vernizzi, JCAP **12**, 025 (2018). arXiv:1809.03484 [astro-ph.CO]
36. S. Hirano, T. Kobayashi, D. Yamauchi, Phys. Rev. D **99**, 104073 (2019). arXiv:1903.08399 [gr-qc]

37. E.J. Copeland, A.R. Liddle, D. Wands, Phys. Rev. D **57**, 4686–4690 (1998). arXiv:gr-qc/9711068

38. P.G. Ferreira, M. Joyce, Phys. Rev. D **58**, 023503 (1998). arXiv:astro-ph/9711102

39. A. Nunes, J.P. Mimoso, Phys. Lett. B **488**, 423–427 (2000). arXiv:gr-qc/0008003

40. C. Rubano, J.D. Barrow, Phys. Rev. D **64**, 127301 (2001). arXiv:gr-qc/0105037

41. Z.K. Guo, Y.S. Piao, Y.Z. Zhang, Phys. Lett. B **568**, 1–7 (2003). arXiv:hep-th/0304048

42. Z.K. Guo, Y.S. Piao, R.G. Cai, Y.Z. Zhang, Phys. Lett. B **576**, 12–17 (2003). arXiv:hep-th/0306245

43. A. De Felice, S. Tsujikawa, JCAP **03**, 025 (2012). arXiv:1112.1774 [astro-ph.CO]

44. L. Amendola, D. Bettoni, G. Domenech, A. Gomes, JCAP **06**, 029 (2018). arXiv:1803.06368 [gr-qc]

45. F. Piazza, S. Tsujikawa, JCAP **07**, 004 (2004). arXiv:hep-th/0405054

46. S. Tsujikawa, M. Sami, Phys. Lett. B **603**, 113–123 (2004). arXiv:hep-th/0409212

47. L. Amendola, M. Quartin, S. Tsujikawa, I. Waga, Phys. Rev. D **74**, 023525 (2006). arXiv:astro-ph/0605488

48. Y. Gong, A. Wang, Y.Z. Zhang, Phys. Lett. B **636**, 286–292 (2006). arXiv:gr-qc/0603050

49. N. Frusciante, R. Kase, K. Koyama, S. Tsujikawa, D. Vernieri, Phys. Lett. B **790**, 167–175 (2019). arXiv:1812.05204 [gr-qc]

50. D. Langlois, M. Mancarella, K. Noui, F. Vernizzi, JCAP **05**, 033 (2017). arXiv:1703.03797 [hep-th]

51. D. Langlois, R. Saito, D. Yamauchi, K. Noui, Phys. Rev. D **97**, 061501 (2018). arXiv:1711.07403 [gr-qc]

52. C. de Rham, A. Matas, JCAP **06**, 041 (2016). arXiv:1604.08638 [hep-th]

53. M. Crisostomi, K. Koyama, Phys. Rev. D **97**, 084004 (2018). arXiv:1712.06556 [astro-ph.CO]

54. M. Zumalacárregui, J. García-Bellido, Phys. Rev. D **89**, 064046 (2014). arXiv:1308.4685 [gr-qc]

55. C. van de Bruck, T. Koivisto, C. Longden, JCAP **03**, 006 (2016). arXiv:1510.01650v2 [astro-ph.CO]

56. S. Sapa, K. Karwan, D.F. Mota, Phys. Rev. D **98**, 23528 (2018). arXiv:1803.02299 [astro-ph.CO]